



Structural and electromechanical study of $\text{Bi}_{0.5}\text{Na}_{0.5}\text{TiO}_3\text{-BaTiO}_3$ solid-solutions

Biswanath Parija¹, Tanmaya Badapanda^{2,*}, Pratap Kumar Sahoo³, Manoranjan Kar⁴, Pawan Kumar⁵, Simanchalo Panigrahi⁵,

¹Department of Physics, Gandhi Engineering College, Bhubaneswar, Odisha 752054, India

²Department of Physics, CV Raman College of Engineering, Bhubaneswar-752054, India

³Department of Physics, National Institute of Science Education and Research (NISER), Bhubaneswar, Odisha 751005, India

⁴Department of Physics, Indian Institute of Technology, Patna- 800013, India

⁵Department of Physics, National Institute of Technology, Rourkela-769008, India

Received 10 April 2013; received in revised form 13 Juni 2013; accepted 18 Juni 2013

Abstract

Solid solution of $(1-x)\text{Bi}_{0.5}\text{Na}_{0.5}\text{TiO}_3-x\text{BaTiO}_3$ have been synthesized via conventional solid-state reaction route. Structural changes of the solid-solutions were investigated by using X-ray diffraction, Rietveld refinement Raman spectroscopy and piezoelectric studies. X-ray diffraction analysis shows a distinct 002/200 peak splitting appearing at $x = 0.07$ showing the coexistence of rhombohedral and tetragonal phase. Raman spectroscopy shows a splitting of (TO3) mode at $x = 0.07$ confirming the presence of the morphotropic phase boundary region. The dominant bands in the Raman spectra are analysed by observing the changes in their respective peak positions, widths and intensities as the x increases. The piezoelectric properties of the solid solution increase with rise in BaTiO_3 content and shows optimum value at $x = 0.07$ owing to the co-existence of two ferroelectric phases. Based on these results, it is suggested that the morphotropic phase boundary in the studied system lies in the composition $x = 0.07$.

Keywords: $\text{Bi}_{0.5}\text{Na}_{0.5}\text{TiO}_3$, BaTiO_3 , solid-solutions, Reitveld refinement, Raman spectroscopy, electromechanical study

I. Introduction

Bismuth sodium titanate $\text{Bi}_{0.5}\text{Na}_{0.5}\text{TiO}_3$ (BNT) is one of the highly studied lead-free perovskite compounds for the replacement of lead-based piezoelectric ceramics on account of their potential electromechanical properties. $\text{Bi}_{0.5}\text{Na}_{0.5}\text{TiO}_3$ and its solid solutions with other perovskites can have good piezoelectric properties and thus are considered to be the potential candidates for industrial applications. The intriguing phase transitions of both BNT and BNT-based solid-solutions as a function of composition and temperature make them an excellent model for studies on the phase transition behaviour [1–4]. Pure BNT is an A-site complex perovskite-structured ferroelectric with rhombohe-

dral symmetry at room temperature. It has a high Curie temperature ($T_c = 320$ °C) with strong ferroelectricity ($P_r = 38$ $\mu\text{C}/\text{cm}^2$) [5–7]. However, the major drawback with BNT is the poling treatment because of its high coercive field ($E_c = 7.3$ kV/mm), resulting in relatively weak piezoelectric properties ($d_{33} = 70\text{--}80$ pC/N). Decreasing coercive field and improving the poling process formation of BNT-based solid solution with a morphotropic phase boundary (MPB) is an effective way as proposed and studied by many researchers.

Recently many binary or ternary BNT-based MPBs have been reported in literature [11–18]. Among them $(1-x)\text{Bi}_{0.5}\text{Na}_{0.5}\text{TiO}_3-x\text{BaTiO}_3$ ceramic system has been well studied [19]. BaTiO_3 (BT) is one of the most investigated classical ferroelectric materials having high dielectric constant, piezoelectric coefficient, electro-optic coefficients, broad wavelength sensitivity range,

* Corresponding author: tel: +91 943 7306100
fax: +91 661 2462022, e-mail: badapanda.tanmaya@gmail.com

high crystalline uniformity, and it displays a large variety of nonlinear optical effects. It was anticipated that the structure of the solid-solution with a low BT content would become tetragonal due to the rather large lattice distortion of BT compared to the rhombohedral distortion in BNT. Although this structural modification was conformed in earlier works, exclusive studies regarding MPB are rare in the literature [20–24]. Rietveld refinements, Raman spectroscopy and piezoelectric studies have been used as effective techniques to investigate the structural evolution in perovskite solid-solutions. Only, limited reports are available on Raman spectroscopy studies but Rietveld refinements are not well reported in BNT-based systems [25–27]. The present manuscript reports the detailed structural study (X-ray diffraction, Rietveld refinement, Raman spectroscopy) and piezoelectric behaviour by electromechanical factors.

II. Experimental

The samples were prepared by a conventional mixed oxide process. In the first step $\text{Bi}_{0.5}\text{Na}_{0.5}\text{TiO}_3$ (BNT) and BaTiO_3 (BT) master batches were made from Bi_2O_3 (99.9%), Na_2CO_3 (99.9%), BaCO_3 (99.9%), and TiO_2 (99.9%). Appropriate amount of reagents was mixed in a Zirconia medium for 12 h using a laboratory designed ball milling unit. The BNT sample was calcined at 700 °C for 4 h and at 850 °C for 2 h with intermediate grinding and mixing. The BT sample was calcined at 1000 °C for 4 h and at 1250 °C for 4 h with intermediate grinding and mixing. The phase purity of both the master samples was investigated using X-ray diffraction (XRD), (Xpert MPD, Philips, UK). Appropriate amount of BNT and BT was mixed thoroughly and sintered at 1150 °C to obtain $(1-x)\text{Bi}_{0.5}\text{Na}_{0.5}\text{TiO}_3-x\text{BaTiO}_3$ (BNT-BT) ceramics. The phase solubility of the compositions was investigated using XRD and Raman spectroscopy

(Enwave Optronics-Ezraman). The prepared ceramic samples were polarized at room temperature under 35 kV/cm in silicone oil for 20 min. The piezoelectric coefficients d_{33} of the samples were measured using a quasi-static piezoelectric d_{33} -meter (YE2730A, China). The impedance (Z) and phase (θ) versus frequency with steps in the range 100 Hz to 1 MHz were measured using Hioki 3532 impedance-phase gain analyser. The resonant and anti-resonant frequencies for the planar vibration modes used to calculate the planar coupling coefficient (K_p) mechanical quality factor (Q_m) and the frequency constant (N_p) by the following equations:

$$K_p = \left[\frac{0.395 \cdot f_r}{(f_a - f_r) + 0.574} \right]^{\frac{1}{2}} \quad (1)$$

$$Q_m = f_a^2 \left[2\pi \cdot R_f \cdot C \cdot f_r (f_a^2 - f_r^2) \right]^{-1} \quad (2)$$

$$N_p = \left(\frac{\pi \cdot d}{3.4} \right) \cdot f_r \quad (3)$$

where f_r and f_a are resonant and anti-resonant frequencies, R_f , C and d are resonant impedance, electrical capacitance and diameter of the pellet, respectively.

III. Results and discussion

3.1 X-ray diffraction

Figure 1a shows the XRD patterns of $(1-x)\text{Bi}_{0.5}\text{Na}_{0.5}\text{TiO}_3-x\text{BaTiO}_3$ ceramics with $0 \leq x \leq 0.08$ sintered at 1150 °C for 4 h. All the compositions exhibit a pure perovskite structure and no second phases are observed, which implies that BaTiO_3 (BT) ceramic has diffused into the $\text{Bi}_{0.5}\text{Na}_{0.5}\text{TiO}_3$ lattices to form a solid-solution. Also Fig. 1b shows the XRD patterns of the ceramics in the 2θ range of 44–50 degree. A distinct 002/200 peak splitting appears when $x = 0.07$, refer-

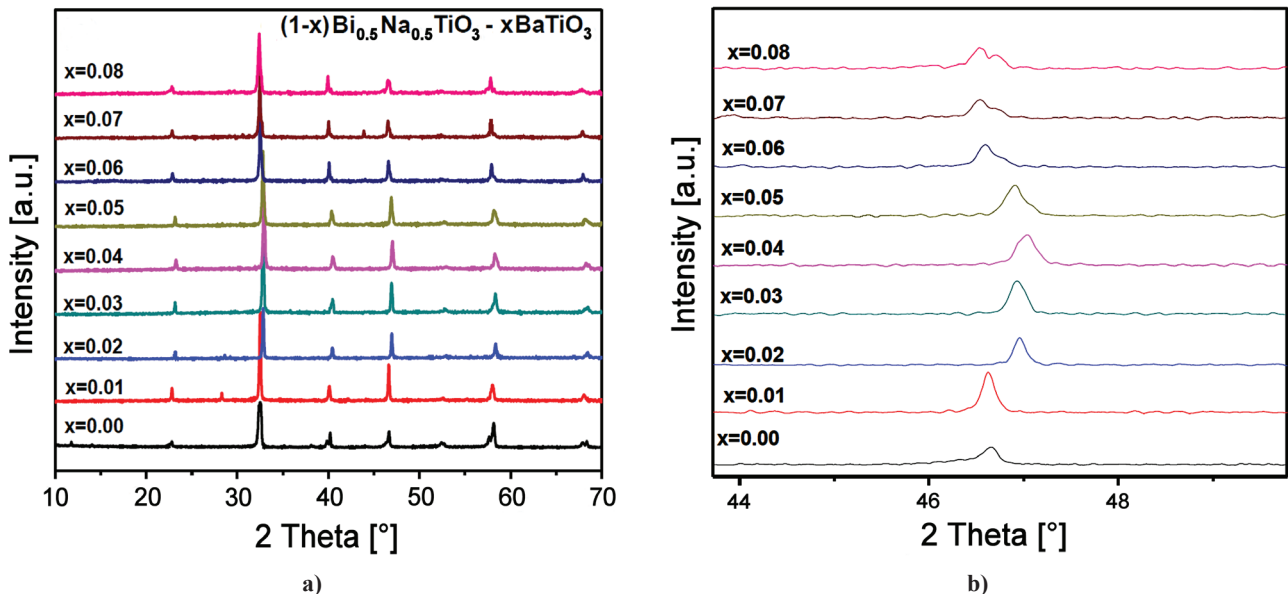


Figure 1. XRD patterns of $(1-x)\text{Bi}_{0.5}\text{Na}_{0.5}\text{TiO}_3-x\text{BaTiO}_3$ ceramic

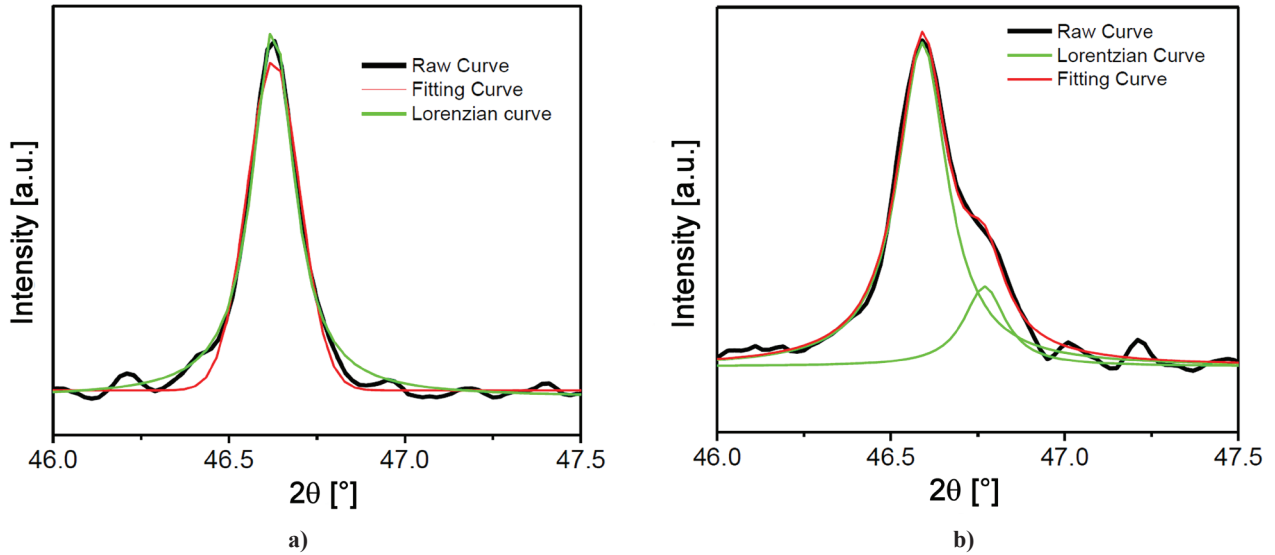


Figure 2. XRD fitting patterns of (1-x)NBT-xBT ceramics with (a) $x = 0$, (b) $x = 0.07$

ring to a tetragonal symmetry. To characterize the phase compositions in a more quantitative way, the XRD patterns of the MPB compositions in the 2θ ranges of 46–48 ° were fitted as shown in Fig. 2. The data show the Lorentzian deconvolution of the 002 and 200 peaks of the tetragonal phase and the 202 peak of the rhombohedral phase. These results suggest that the rhombohedral-tetragonal morphotropic phase boundary (MPB) of (1-x)NBT-xBT ceramic is near $x = 0.07$.

The detailed crystal structure has been studied by analysing XRD patterns recorded at room temperature using Rietveld method and Fullprof software. The pseudo-Voigt function was used to define the peak profiles while a fifth-order polynomial was used for describing the background. It is observed that the difference between the profiles of the XRD patterns experimentally observed and theoretically calculated display small difference as illustrated by a line ($Y_{Observed} - Y_{Calculated}$). The fitting parameters (R_{wrb} , R_b , R_{exp} , R_w , and σ) suggest that the refinement results are well-reliable. Tables 1 and 2 summarize the Rietveld-refinement result carried out

in the MPB composition of BNT-BT solid-solutions, where the setting parameters of $R3c$ were referred to Corker *et al.* [28] and those of $P4mm$ were set according to the crystallographic limitation of its space group. Replacing the refined phase by the coexisting rhombohedral and tetragonal phases resulted in a good fitting between the observed intensities and the calculated intensities of $0.93\text{Bi}_{0.5}\text{Na}_{0.5}\text{TiO}_3-0.07\text{BaTiO}_3$. The result indicates that 0.93BNT-0.07BT is composed of 41.2% rhombohedral phase and 58.8% tetragonal phase, so that 0.93BNT-0.07 BT is confirmed to be a MPB composition.

3.2 Microstructure

Figure 3 shows the SEM micrograph of natural surface for (1-x) $\text{Bi}_{0.5}\text{Na}_{0.5}\text{TiO}_3-x\text{BaTiO}_3$ ceramics. The pure BNT sample presents rectangular grain morphology while the BT addition changes the grain shape to spherical shape. All sample surface grains present regular geometry with compact structure. BNT disk appears to be poly-dispersed in both size and shape due to inhomogeneous grain growth. On the contra-

Table 1. Rietveld-refinement results and atomic coordinates of $0.93\text{Bi}_{0.5}\text{Na}_{0.5}\text{TiO}_3-0.07\text{BaTiO}_3$ ceramics (MPB region)

Phase	Atom	X	Y	Z	Biso
Rhombohedral <i>R3c</i>	Bi	0	0	0.2903(13)	0.3840(18)
	Ba	0	0	0.2903(13)	0.3840(18)
	Na	0	0	0.2903(13)	0.3840(18)
	Ti	0	0	0.0177(14)	0.2840(19)
	O1	0.1596(15)	0.3297(16)	0.8866(17)	0.9834(20)
Tetrahedral <i>P4mm</i>	Bi	0	0	0	0.3201(16)
	Ba	0	0	0	0.3201(16)
	Na	0	0	0	0.3201(16)
	Ti	0.5	0.5	0.5356	0.2485(17)
	O1	0.5	0.5	-0.10931	0.5447(18)
	O2	0.5	0	0.41957	0.0374(19)

The reliability factors are $R_p = 10.25\%$, $R_{wp} = 10.8\%$, $\chi = 2.54$, $R_{exp} = 11.5\%$ and $R_{Bragg} = 8.1\%$

Table 2. Refinement results (phase percentage, cell parameter and cell volume) of the crystal structure of $0.93\text{Ba}_{0.5}\text{Na}_{0.5}\text{TiO}_3\text{-}0.07\text{BaTiO}_3$ ceramics

x	Crystal system	Space group	Phase [%]	Lattice parameters		Cell volume [\AA^3]
				a [\AA]	c [\AA]	
0.07	Rhombohedral	$R3c$	41.2	5.5201(3)	13.5229(5)	59.4(6)
	Tetragonal	$P4mm$	58.8	3.9025(5)	3.9048(3)	356.8(9)

ry, the addition of BT results in the inhibition of grain growth, so the BNT-BT appears to be more uniform in both size and shape. It can also be seen that the grain size reduces with increase in BT content which is may be due to the Ba^{2+} abundance in crystal boundary preventing the ion from migrating and restrains the growing of grains.

3.3 Raman spectroscopy:

Figure 4 represents the Raman spectroscopy study of $(1-x)\text{Bi}_{0.5}\text{Na}_{0.5}\text{TiO}_3\text{-}x\text{BaTiO}_3$ solid solution ($x = 0.0\text{--}0.08$). There are only five Raman-active modes observed in the range from 100 to 1000 cm^{-1} in agreement with the works reported by the Rout *et al.* [29] and Eerd *et al.* [30]. BNT ceramics with rhombohedral structure presents 13 Raman-active modes ($\Gamma_{\text{Raman}} = 4A1 + 9E$) due to the disorder in A-site related to distorted octahedral $[\text{BiO}_6]$ and $[\text{NaO}_6]$ clusters [31]. The first Raman-active A1 (TO1) mode at around (146 cm^{-1}) is related to network modifiers or distorted octahedral $[\text{BiO}_6]$ and $[\text{NaO}_6]$ clusters. The second Raman active E (TO2) mode can be deconvoluted in three Raman peaks in the regions of 279 cm^{-1} . This mode is assigned to stretching arising from the bonds due to presence of octahedral $[\text{TiO}_6]$ clusters at short-range. The third Raman-active (LO2) mode with low intensity is related to short-range electrostatic forces associated with the lattice ionicity [32]. According to Dobal *et al.* [33], the (TO3) mode situated at around 542 cm^{-1} is ascribed to the (O–Ti–O) stretching symmetric vibrations of the octahedral $[\text{TiO}_6]$ clusters. The (LO3) mode found at 812 cm^{-1} is due to

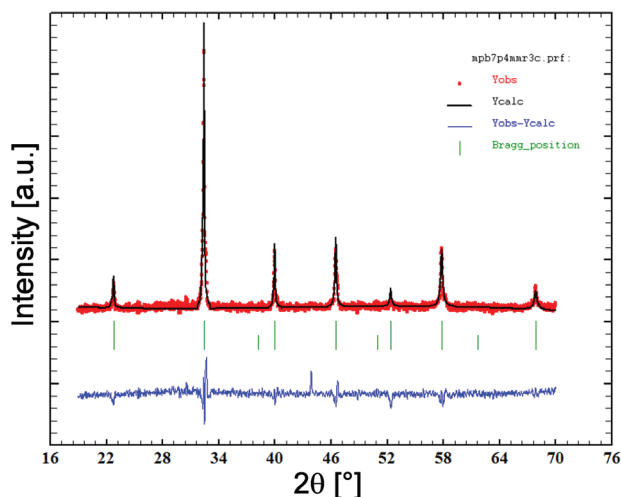


Figure 3. Rietveld refinement plots of $0.93\text{Bi}_{0.5}\text{Na}_{0.5}\text{TiO}_3\text{-}0.07\text{BaTiO}_3$ ceramics

the presence of the sites within the rhombohedral lattice pre containing octahedral distorted $[\text{TiO}_6]$ clusters. These modes are classified into longitudinal (LO) and transverse (TO) components because of the electronic structure with polar character of lattice. There is no significant change in the spectra for the compositions of lower x values (< 0.06). However, the further addition of BT ($x = 0.07$) in the solid solution results in anomaly by splitting bands that shift apart from each other.

For better observation of the Raman spectra of BNT and BNT-BT ($x = 0.07$) along with the curves fitted to individual peaks are shown in Fig. 6. The spectra of BNT-BT ($x = 0.07$) show additional peaks around 145, 280, 545 and 800 cm^{-1} compared to the peaks observed in BNT. The occurrence of these new bands, observed band splitting, indicates a structural change at $x > 0.06$, which are well in line with the studies of XRD phase analysis. All bands appearing in the spectra at $x > 0.06$ can be assigned to the Raman modes for a tetragonal symmetry [34].

However, from Fig. 5 it is possible to detect that all the Raman peaks are very broad in BNT and BNT-BT ceramics. It is believed that this behaviour is due to the presence of the disorder structural or distorted octahedral $[\text{TiO}_6]$ clusters at short-range and the overlapping of Raman modes due to the lattice anharmonicity. For closer investigation, the variation of full width of half maximum (FWHM) and intensity of individual peaks are plotted in Fig. 7. The mode intensity and FWHM undergo slope change at $x = 0.07$. The FWHM of a Raman band is inversely proportional to the lifetime of the corresponding phonon [35], which is in turn closely related to the size of the local $(\text{Bi}_{0.5}\text{Na}_{0.5})^{2+}\text{TiO}_3$ clusters. When Ba^{2+} substitutes for both Bi and Na, $\text{Ba}^{2+}\text{TiO}_3$ clusters are formed. As a result, $(\text{Bi}_{0.5}\text{Na}_{0.5})^{2+}\text{TiO}_3$ clusters are reduced in sizes, giving rise to the peak broadening and intensity weakening of the 280 cm^{-1} band. There is no change in the frequency of this band since both composition and structure remain the same in the $(\text{Bi}_{0.5}\text{Na}_{0.5})^{2+}\text{TiO}_3$ clusters when x values are low. With the increase in x value such constraining effect becomes less significant and the phase transition occurs. The variation of intensity and FWHM of all peaks shows a similar type of anomaly at $x = 0.07$. On the basis of these considerations, it is possible to conclude that the rhombohedral-tetragonal phase co-exists at $x = 0.07$ which is also observed in the XRD results.

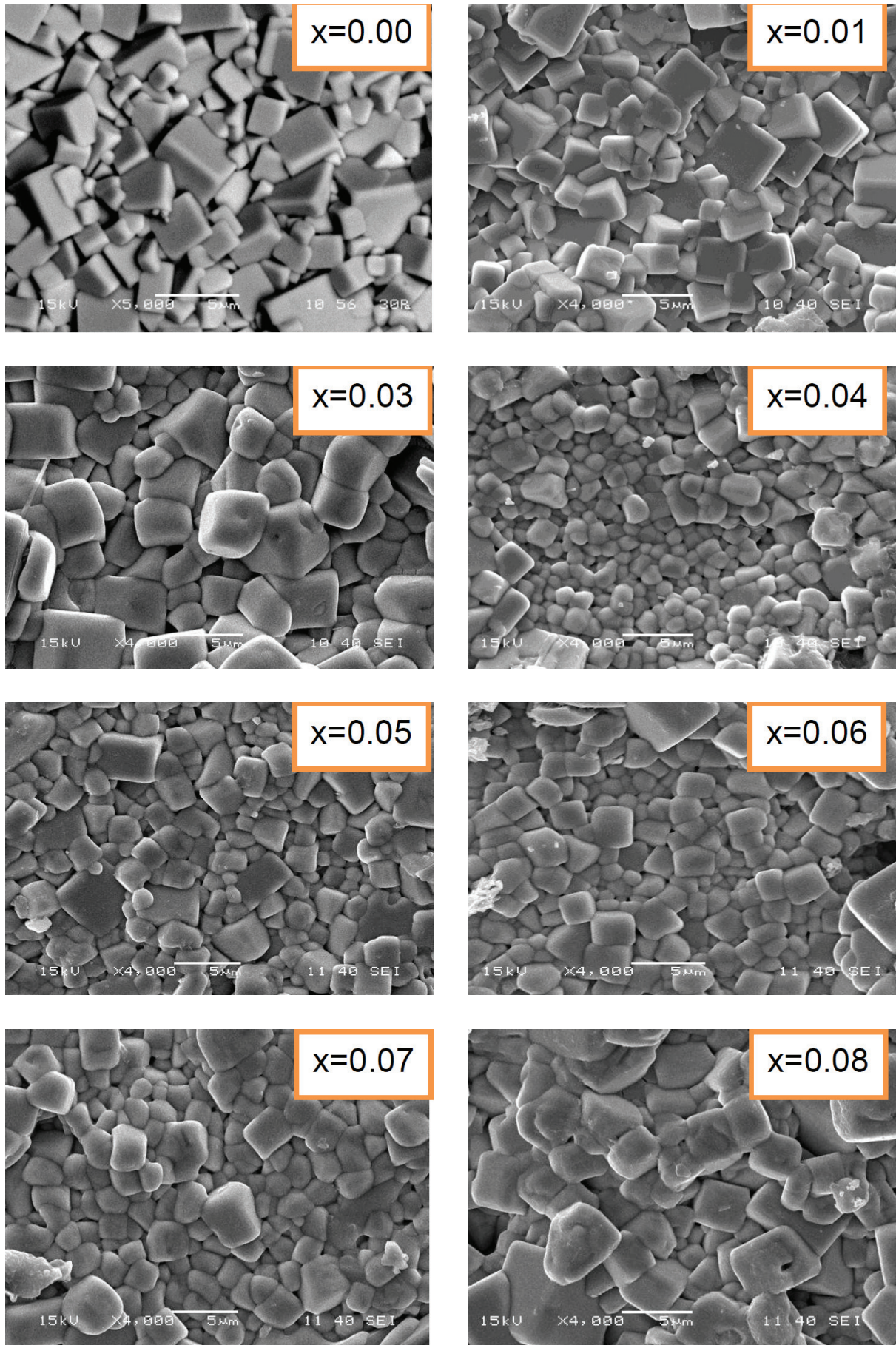


Figure 4. Microstructure of $(1-x)\text{Bi}_{0.5}\text{Na}_{0.5}\text{TiO}_3-x\text{BaTiO}_3$ ceramics ($0 \leq x \leq 0.08$)

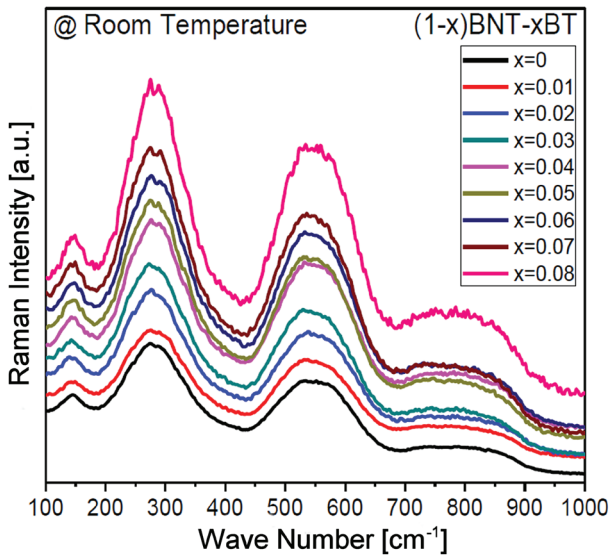
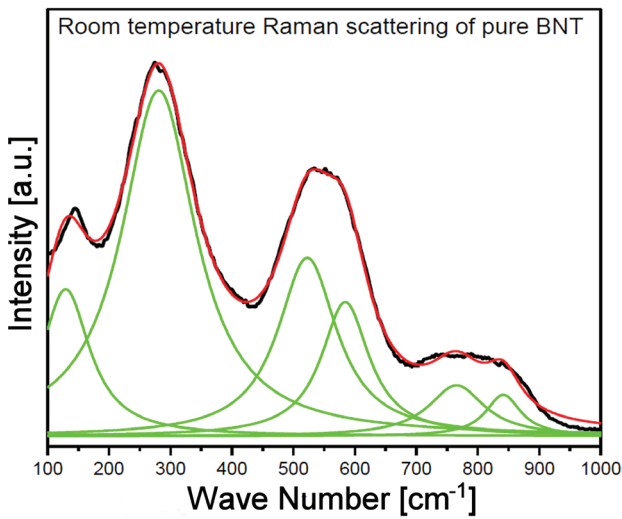


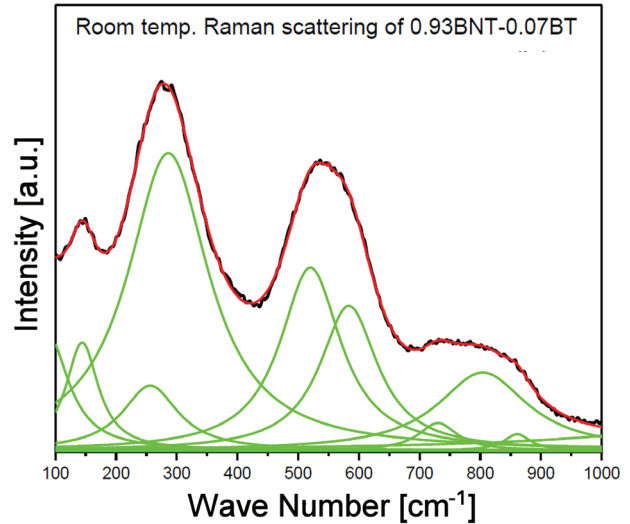
Figure 5. Room temperature Raman spectrum of (1-x)BNT-xBT ($0 \leq x \leq 0.08$)

3.4 Piezoelectric and electromechanical study

The various piezoelectric and electromechanical parameters are obtained from the equations (1), (2) and (3) described above. The resonance and anti-resonance frequencies were found from the impedance and phase analysis. Figure 8 shows the frequency versus impedance / phase spectra of the BNT-BT solid-solution at $x = 0.07$ composition. It is observed that the piezoelectric properties strongly exhibit a compositional dependence. The piezoelectric constant d_{33} and electromechanical coupling factor K_p display a similar variation, enhancing with the increasing of x , attains a maximum value in a composition $x = 0.07$ and then tending to decrease. The piezoelectric constant d_{33} attains a maximum value of 131 pC/N and the electromechanical coupling factor K_p reaches the maximum value of 45% at $x = 0.07$ shown in Fig. 9a. The increase in the piezoelectric constant d_{33} in the MPB composition may be

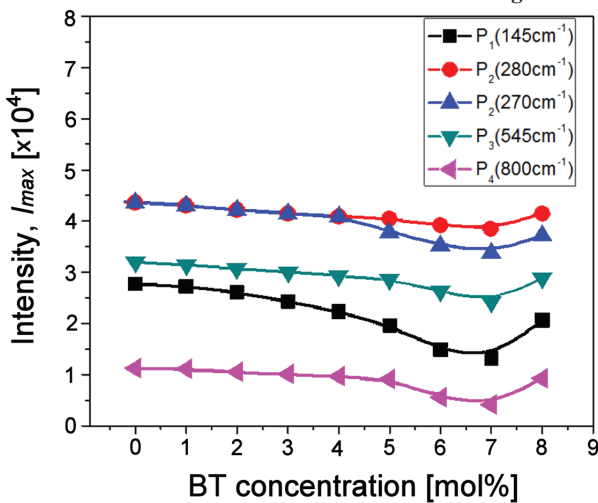


a)

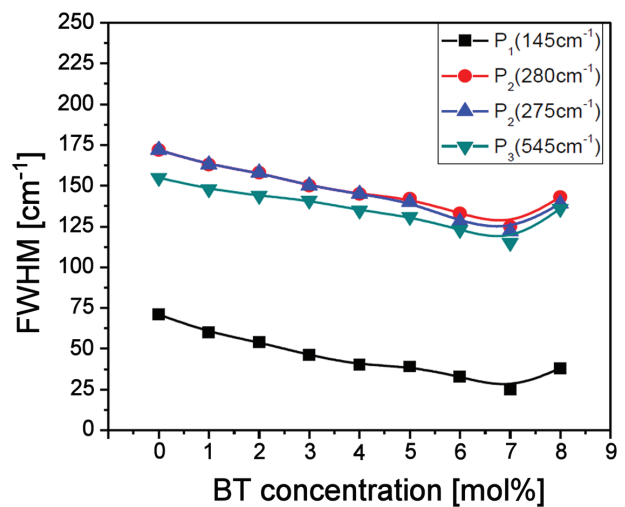


b)

Figure 6. Raman spectra of BNT and $0.93\text{Bi}_{0.5}\text{Na}_{0.5}\text{TiO}_3-0.07\text{BaTiO}_3$. Black line is the experimental data and green lines are the fitting curve versus BT concentration



a)



b)

Figure 7. Variation of the intensity (a) and FWHM (b) of different modes in the Raman spectra versus BT concentration

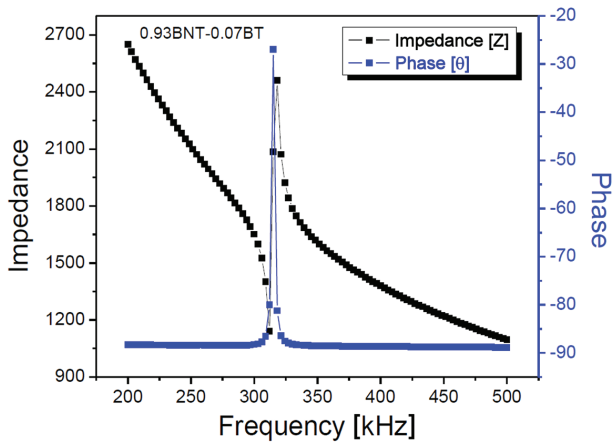


Figure 8. The frequency vs. impedance / phase spectrum of 0.93BNT-0.07BT ceramic (MPB composition)

attributed to an increase in the domain wall flexibility. The ceramic crystal structure is considered to be a co-existence of rhombohedral and tetragonal phases in the MPB composition. As the rhombohedral phase free energy is close to the tetragonal phase free energy, these two phases are easily exchanged by applying an electric field. In a close vicinity of MPB both crystallographic phases are in thermal equilibrium with each other with vanishing polarization anisotropy. Therefore, a flipping of polarization between two phases is possible under applied electric field. Enhanced piezoelectric coefficients are obtained in MPB regions and are attributed to an easy switch in the polarization vector between all allowed polarization orientations [36,37]. It can be seen that mechanical quality factor Q_m of the specimens decreases with increasing x amount, reaches the minimum value at $x = 0.07$ and then shows a slight increase with rise in x value. A similar kind of behaviour is also observed for frequency constant (N_p) of the specimens as seen in Fig. 9b. Compared with ordinary sintered BNT ceramics, BNT-BT ceramics show enhanced piezoelectric and electromechanical properties which demon-

strate that BNT-BT ceramics near the MPB are promising piezoelectric materials for lead-free applications. The piezoelectric and electromechanical properties also confirm that the morphotropic phase boundary exists near $x = 0.07$.

IV. Conclusions

The solid-solutions $(1-x)\text{Bi}_{0.5}\text{Na}_{0.5}\text{TiO}_3-x\text{BaTiO}_3$ were successfully synthesized by a conventional solid state reaction rout. X-ray diffraction and Rietveld refinement analysis showed that a morphotropic phase boundary (MPB) exists around $x = 0.07$. Analysis of peak positions, widths and intensities of Raman spectroscopy study also confirmed the existence of morphotropic phase boundary around $x = 0.07$ composition. The piezoelectric study shows enhancement with an increase in BT content and maximum at $x = 0.07$. The electromechanical behaviour shows optimum results at $x = 0.07$ confirming the MPB. Both the structural and electrical properties show that the solid solution has a MPB around $x = 0.07$ which is expected to be a new and promising candidate for lead-free dielectric and piezoelectric material.

References

1. J.K. Lee, K.S. Hong, C.K. Kim, S.E. Park, "Phase transitions and dielectric properties in A-site ion substituted $(\text{Na}_{1/2}\text{Bi}_{1/2})\text{TiO}_3$ ceramics (A = Pb and Sr)", *J. Appl. Phys.*, **91** (2002) 4538–4543.
2. S.E. Park, K.S. Hong, "Phase relations in the system of $(\text{Na}_{1/2}\text{Bi}_{1/2})\text{TiO}_3\text{-PbTiO}_3$. I. Structure", *J. Appl. Phys.*, **79** (1996) 383–388.
3. J. Kreisel, A.M. Glazer, P. Bouvier, G. Lucazeau, "High-pressure Raman study of a relaxor ferroelectric: The $\text{Na}_{0.5}\text{Bi}_{0.5}\text{TiO}_3$ perovskite", *Phys. Rev. B*, **63** (2001) 174106-116.
4. O. Elkechai, P. Marchet, P. Thomas, M. Manier, J.P. Mercurio, "Phase transitions in A-site substituted perovskite compounds", *J. Mater. Chem.*, **7** (1997) 91–97.

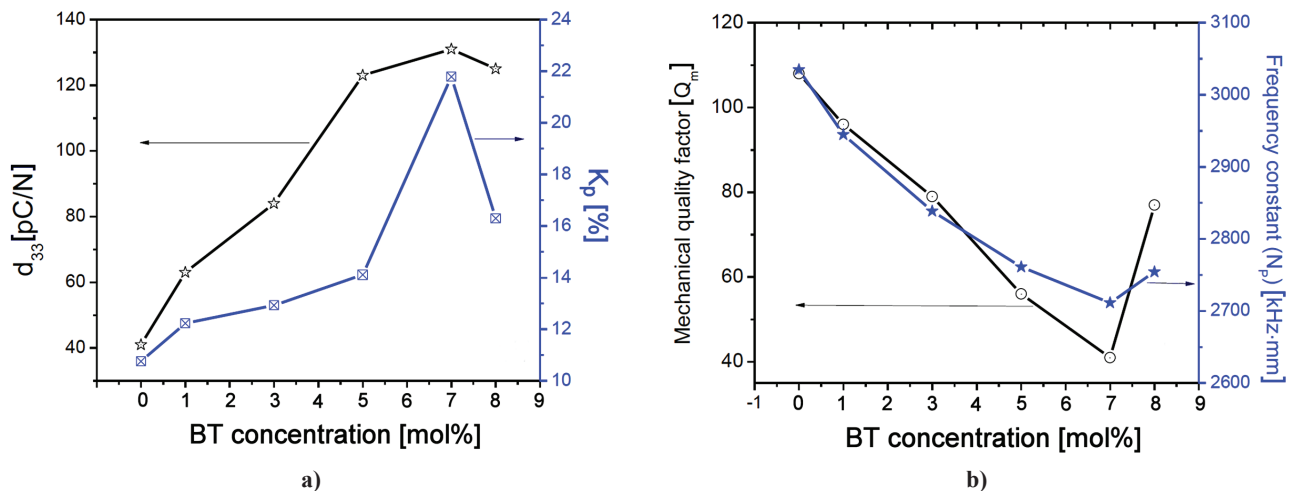


Figure 9. Piezoelectric co-efficient (d_{33}) and electromechanical coupling factor (k_p) (a) and mechanical quality factor (Q_m) and frequency constant (N_p) (b) of BNT-BT ceramics versus BT concentration

5. M.H. Frey, D.A. Payne, “Grain-size effect on structure and phase transformations for barium titanate”, *Phys. Rev. B*, **54** (1996) 3158–3168.
6. M. Yashima, T. Hoshina, D. Ishimura, S. Kobayashi, W. Nakamura, T. Tsurumi, S. Wada, “Grain-size effect on structure and phase transformations for barium titanate”, *J. Appl. Phys.*, **98** (2005) 014313.
7. T. Yamamoto, K. Urabe, H. Banno, “BaTiO₃ particle-size dependence of ferroelectricity in BaTiO₃/polymer composites”, *Jpn. J. Appl. Phys.*, **32** (1993) 4272–4276.
8. X. Li, W.-H. Shih, “Size effects in barium titanate particles and clusters”, *J. Am. Ceram. Soc.*, **80** (1997) 2844–2896.
9. B.D. Begg, E.R. Vance, J. Nowotny, “Effect of particle size on the room-temperature crystal structure of barium titanate”, *J. Am. Ceram. Soc.*, **77** (1994) 3186–3192.
10. Y.M. Chiang, G.W. Farrey, A.N. Soukhovjak, “Lead-free high-strain single-crystal piezoelectrics in the alkaline-bismuth-titanate perovskite family”, *Appl. Phys. Lett.*, **73** (1998) 3683–3685.
11. J.R.G. Pettry, S. Said, P. Marchet, J.P. Mercuro, “Crystal structure and properties of BaTiO₃-(Bi_{0.5}Na_{0.5})TiO₃ ceramic system”, *J. Eur. Ceram. Soc.*, **24** (2004) 1165–1169.
12. T. Takenaka, K. Maruyama, K. Sakata, “(Bi_{1/2}Na_{1/2})TiO₃-BaTiO₃ system for lead-free piezoelectric ceramics”, *J. Appl. Phys.*, **30** (1991) 2236–2239.
13. Y. Hosono, K. Harada, Y. Yamashita, “Crystal growth and electrical properties of lead-free piezoelectric material (Na_{1/2}Bi_{1/2})TiO₃-BaTiO₃”, *Jpn. J. Appl. Phys.*, **40** (2001) 5722–5726.
14. B.J. Chu, D.R. Chen, G.R. Li, Q.R. Yin, “Electrical properties of Na_{1/2}Bi_{1/2}TiO₃-BaTiO₃ ceramics”, *J. Eur. Ceram. Soc.*, **22** (2002) 2115–2121.
15. D. Rout, K.S. Moon, V.S. Rao, S.J.L. Kang, “Study of the morphotropic phase boundary in the lead-free Na_{1/2}Bi_{1/2}TiO₃-BaTiO₃ system by Raman spectroscopy”, *J. Ceram. Soc. Jpn.*, **117** [7] (2009) 797–800.
16. K. Pengpat, S. Hanphimol, S. Eitsayeam, U. Intatha, G. Rujijanagul, T. Tunkasiri, “Morphotropic phase boundary and electrical properties of lead-free bismuth sodium lanthanum titanate-barium titanate ceramics”, *J. Electroceram.*, **16** (2006) 301–305.
17. W. Jo, J.E. Daniels, J.L. Jones, X. Tan, P.A. Thomas, D. Damjanovic, J. Rödel, “Evolving morphotropic phase boundary in lead-free Bi_{1/2}Na_{1/2}TiO₃-BaTiO₃ piezoceramics”, *J. Appl. Phys.*, **109** (2011) 014110.
18. I.G. Siny, E. Husson, J.M. Beny, S.G. Lushnikov, E.A. Rogacheva, P.P. Syrnikov, “Raman scattering in the relaxor-type ferroelectric Na_{1/2}Bi_{1/2}TiO₃”, *Ferroelectrics*, **248** (2000) 57–78.
19. J. Kreisel, A.M. Glazer, G. Jones, P.A. Thomas, L. Abollo, G. Lucazeau, “An X-ray diffraction and Raman spectroscopy investigation of A-site substituted perovskite compounds: The (Na_{1-x}K_x)_{0.5}Bi_{0.5}TiO₃ solid solution”, *J. Phys: Condens. Matter*, **12** (2000) 3267–3280.
20. S. Trujillo, J. Kreisel, Q. Jiang, J.H. Smith, A.P. Thomas, P. Bouvier, F. Weiss, “The high-pressure behaviour of Ba-doped Na_{1/2}Bi_{1/2}TiO₃ investigated by Raman spectroscopy”, *J. Phys: Condens. Matter*, **17** (2005) 6587–6597.
21. J. Wang, Z. Zhou, J. Xue, “Phase transition, ferroelectric behaviors and domain structures of (Na_{1/2}Bi_{1/2})_{1-x}TiPb_xO₃ thin films”, *Acta Materials*, **54** (2006) 1691–1698.
22. D.L. Corker, A.M. Glazer, R.W. Whatmore, A. Stalard, F. Rauth, “A neutron diffraction investigation into rhombohedral phases of the perovskite series PbZr_{1-x}Ti_xO₃”, *J. Phys: Condens. Matter*, **10** (1998) 6251–6269.
23. M.S. Zhang, J.F. Scott, “Raman spectroscopy of (Na_{0.5}Bi_{0.5})TiO₃”, *Ferroelectr. Lett.*, **6** (1986) 147–152.
24. A.S. Barker, A.J. Sievers, “Optical studies of the vibrational properties of disordered solids”, *Rev. Mod. Phys.*, **47** (1975) S1–S179 Suppl No 2, 180.
25. J. Kreisel, B. Dkhil, P. Bouvier, J.M. Kiat, “Effect of high pressure on relaxor ferroelectrics”, *Phys. Rev., B*, **65** (2002) 172101-1
26. M.E. Marssi, R. Farhi, X. Dai, A. Morell, D. Viehland, “A Raman scattering study of the ferroelectric ordering in rhombohedral and tetragonal La-modified lead zirconate titanate ceramics”, *J. Appl. Phys.*, **80** (1996) 1079–1084.
27. H. Uwe, K.B. Lyons, H.L. Carter, P.A. Fleury, “Ferroelectric microregions and Raman scattering in KTaO₃”, *Phys. Rev. B*, **33** (1986) 6436–6440.
28. K.S. Hong, S.E. Park, “Phase relations in the system of (Na_{1/2}Ni_{1/2})TiO₃-PbTiO₃. II. Dielectric property”, *J. Appl. Phys.*, **79** (1996) 388–392.
29. S.B. Vakhrushev, V.A. Isupov, B.E. Kvyatkovsky, N.M. Okuneva, I.P. Pronin, “Phase transitions and soft modes in sodium bismuth titanate”, *Ferroelectrics*, **63** (1985) 153–160.